Optimization of Criteria for an Efficient Screening of New Thermoelectric Compounds: The TiNiSi Structure-Type as a Case-Study

Céline Barreteau, Jean-Claude Crivello, Jean-Marc Joubert, Eric Alleno

Optimization of criteria for an efficient screening of new thermoelectric compounds: the TiNiSi structure-type as a case-study

Celine Barreteau[1], Jean-Claude Crivello, Jean-Marc Joubert and Eric Alleno

1 Univ Paris Est Créteil, CNRS, ICMPE, UMR7182, F-94320, Thiais, FRANCE

ABSTRACT

High-throughput calculations can be applied to a large number of compounds, in order to discover new useful materials. In the present work, ternary intermetallic compounds are investigated, to find new potentially interesting materials for thermoelectric applications. The screening of stable non-metallic compounds required for such applications is performed by calculating their electronic structure, using DFT methods. In the first section, the study of the density of states at the Fermi level, of pure elements, binary and ternary compounds, leads to empirically chose the selection criterion to distinguish metals from non-metals. In the second section, the TiNiSi structure-type is used as a case-study application, through the investigation of 570 possible compositions. The screening leads to the selection of 12 possible semiconductors. The Seebeck coefficient and the lattice thermal conductivity of the selected

[1] Corresponding author: barreteau@icmpe.cnrs.fr

compounds are calculated in order to identify the most promising ones. Among them, TiNiSi, TaNiP or HfCoP are shown to be worth a detailed experimental investigation.

KEYWORDS: Thermoelectricity, DFT calculations, Semiconductors, Intermetallic

INTRODUCTION

Thermoelectricity may be used as an interesting technology able to reduce the energy consumption through the recycling of waste heat. The conversion efficiency of thermoelectric devices is related to the dimensionless figure of merit *ZT* of their constituting materials, which is defined as

$$ZT = S^2\sigma T/\kappa \qquad (1)$$

where: S represents the Seebeck coefficient; σ the electrical conductivity; κ the thermal conductivity and T the absolute temperature. Even though efficient thermoelectric devices exist, they are limited to niche markets because of their quite high cost compared to their conversion yield. One way to improve this technology is to find new materials based on more abundant, less toxic and less expensive elements. These limitations led us to define a set of elements, we could investigate to search for new interesting compounds [1]. For this set of elements, hundreds of compounds have already been reported in crystallographic databases, and even if some of them are known to be good thermoelectric compounds, there is still a very large number of possibly unknown compounds. In order to screen more efficiently the possible combinations, we use high-throughput calculations. We will present an efficient method to screen ternary intermetallic compounds in order to find new promising thermoelectric compounds. In this article, we will focus on the equimolar compounds and use the orthorhombic TiNiSi structure type as a case-study. We choose the TiNiSi structure-type because even though it is a large family with more than 70 compounds already reported in the crystallographic databases [2-3], it

has been less subject of investigations compared with other equimolar structure-types. In contrast, numerous high-throughput calculations and screenings have already successfully shown very promising results for the equimolar half-Heusler family [4-8].

Before estimating the thermoelectric properties of the compounds pertaining to the TiNiSi family, the main goal of the present work is to define an efficient method to discriminate among the investigated compounds those, which might be both stable and semiconducting. In our previous investigation [1], we compared the enthalpy of formation of the same combination of elements in four structure types to determine the most stable one. In the present work, for the compounds stable in the TiNiSi structure-type, investigation of the electronic band structure will be carried out, to exclude the metallic compounds and keep only the possible semiconductors and semi-metals. A definition and the application of our exclusion criterion will be presented in this article. For the most remarkable compounds, the Seebeck coefficient and the thermal conductivity will be estimated using calculations based on the BoltzTrap package [9-10] and the Slack equation [11-12] respectively. All the results will be compared with the literature and the selected compounds will be highlighted.

COMPUTATIONAL DETAILS AND METHODOLOGY

In our previous work [1], a combinatorial approach has been implemented to screen all possible *T*-*M*-*X* combinations with the 1:1:1 stoichiometry generated within a restrained set of chemical elements. In this set of elements, *T* is a transition metal from the Ti, V, and Cr columns or Sr, Ba, Y and La. *M* is an element from the first line of transition metals and *X* a *sp* element (Al, P, Si, Sn, and Sb). All *T*-*M*-*X* combinations have been calculated in four different structure-types: the orthorhombic TiNiSi (*Pnma*), the cubic MgAgAs (*F*-43*m*, half-Heusler), the two hexagonal ZrNiAl (*P*-62*m*) and BeZrSi ($P6_3/mmc$). The 570 possible configurations have been calculated in these 4 structure-types by systematically assigning an unique element from our *T*-*M*-*X*

nomenclature to each crystallographic site, discarding "inverse" configurations or site mixing, yielding 2280 different compounds.

The calculations of the stability and ground-state properties are based on the density functional theory (DFT). This technique allows us to obtain the enthalpy of formation at 0 K for each compound (by total energy difference with the elemental reference state) as well as its electronic structure. The calculations were conducted using the projector augmented wave (PAW) method, implemented in the Vienna *Ab initio* Simulation Package (VASP)[13-16]. The exchange correlation was described by the generalized gradient approximation modified by Perdew, Burke, and Ernzerhof (GGA-PBE) [17]. An energy cut-off of 600 eV was used for the plane wave basis set. A high-density *k*-points meshing was employed for Brillouin zone integrations in the TiNiSi structure-type (7 × 11 × 6), MgAgAs (21 × 21 × 21), ZrNiAl (19 × 19 × 37) and BeZrSi (21 × 21 × 10). These parameters ensured robust results in the total energy within convergence tolerance for the calculations set within 10^{-6} eV of difference. We performed volume and ionic relaxation steps for each structure-type, and we considered spin polarization for all the configurations. Blöchl correction was applied in a final step calculation [18]. Phonon dispersion bands were obtained by computing the atomic forces for different, finite atomic displacements [19] and a subsequent calculation and integration over the corresponding phonon frequencies, within the harmonic approximation. i.e. without any volume dependence, using the Phonopy code [20-21]. The phonon calculations were carried out within a 1 × 2 × 1 supercell (24 atoms) with 12 atomic displacements for the TiNiSi structure-type.

The Seebeck coefficient was calculated from the Boltzmann transport theory [22] as implemented in the BoltzTrap simulation package (v2) [9-10]. The BoltzTrap code uses the electronic structure calculated with a dense k-mesh (12 x 20 x 10) from VASP as an input data and assumes a constant relaxation time for the electrons.

The first step of our selection concerns the stability of the calculated compounds. A positive enthalpy of formation leads to the exclusion of the combination, as it is obvious that the ternary compound is unstable toward the decomposition into its pure elements. In the second step, the most negative enthalpy of formation of the four-competing structure-types at the same composition, allows the selection of the most probable stable structure. Comparison with the literature and the crystallographic database has confirmed the robustness of our model [1].

Definition of the non-metallic criterion

In addition to the stability criterion, it is important to find a simple and robust way to exclude metallic compounds for thermoelectric application. For this purpose, we decided to focus our screening method on the density of states (DOS) at the Fermi level (E_F). By definition, when the DOS is zero at the E_F, a semiconducting or insulating ground-state is expected. However, DFT-PBE is known [23-24] to not only systematically underestimate the gap magnitude but also to provide a non-zero DOS for known semiconductors. To compensate for this spurious effect, a non-zero discrimination criterion to select semiconductors is thus required to assess an unknown ground state (not too strict so as to miss interesting compounds and not too high for being efficiently selective). To estimate this value, preliminary calculations have been performed on the chemical elements in their stable structure (table S1) at 0 K and on known semiconducting binary compounds. Most of the elements of the periodic table have been investigated, except the *4f* elements and the noble gas, whereas the investigated binary compounds have been chosen among known semiconductors or semi-metals.

The calculated DOS are presented in Fig. 1. As expected, all the metallic elements (*s, d* blocks) have a non-zero DOS at E_F, consistent with their metallic ground-state. In group ***III***, (B, Al, Ga, In), the last three elements present a non-zero DOS at E_F in agreement with their metallic ground-state whereas B has a zero DOS consistent with its semiconducting ground-state [25].

When looking at the first elements from group ***IV*** (C, Si, Ge), it is obvious that all the DOS at E_F exhibit a zero value. The last two elements of this group, Sn and Pb, have a non-zero DOS at E_F, 0.05 state eV^{-1} by atom and 0.5 state eV^{-1} by atom, respectively. This very low DOS at E_F for Sn agrees with previous results [26] which have shown that "gray tin", the α form of Sn (*A*4), which is the stable allotrope at low temperature [27], is semiconducting. Elemental Pb displays a DOS at E_F similar to the metals of the block *d*. In group ***V*** (P, As, Sb, Bi), P has a zero DOS at E_F whereas As, Sb, and Bi have a DOS smaller than 0.1 state eV^{-1} by atom. This confirms the semi-metallic ground-state of these last three elements, while elemental P is a semiconductor as reported in reference [28]. In group ***VI*** with Se and Te, the DOS at E_F is zero as these elements are reported as semiconductors [29-30]. In addition, all the binary compounds presented in Figure 1 exhibit a zero DOS or a very low DOS at E_F, smaller than 0.005 state eV^{-1} by atom, which is consistent with their semiconducting ground states.

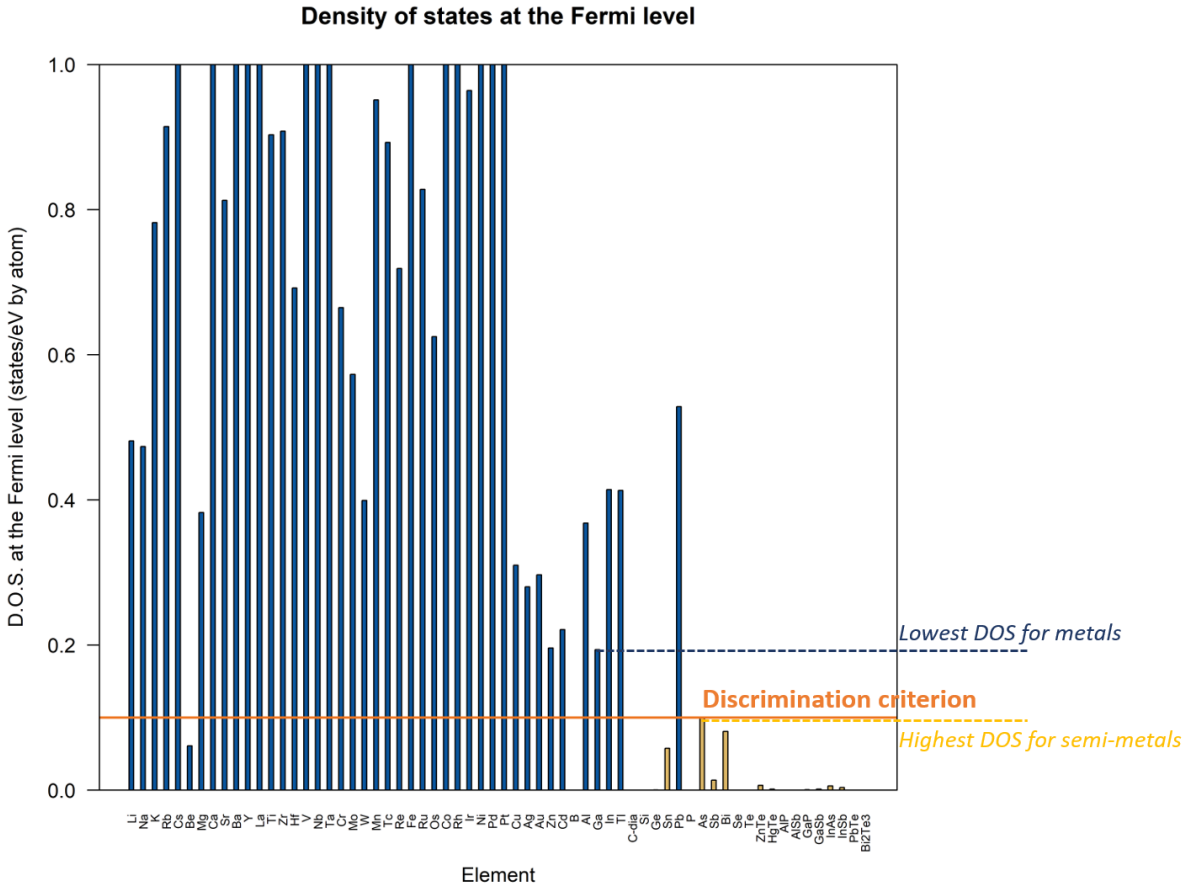

Figure 1. Density of states (DOS) at E_F for a selection of pure elements and binary compounds; reported semiconductors and semi-metals are in yellow and metals are in blue.

Reported results in Figure 1 allow to show an interval between the DOS at E_F for known semiconductor or semi-metallic elements such as Sn or As and these of Ga and Zn, two metallic elements. Thus, with a selection limit set at 0.1 state eV^{-1} by atom for the DOS at E_F, semiconductors, as well as elements with a semi-metallic ground state such as As or Sb, are kept whereas metals are excluded. Only one exception to this criterion is found: with this limit, Be, which is known as a metal is also selected. However, Be is known to exhibit a very low DOS at E_F, despite its metallic behaviour [31-34]. Overall, this limit ensures a judicious selection with a very small number of ambiguous results.

These calculations on elemental and known binary semiconductors allowed to establish an empirical discrimination criterion. However, before using it to screen unknown compounds, an additional test has been made on reported compounds from the Heusler family (full and half-Heusler). This family has been chosen because it has already been the object of several studies [4-5, 35], Heusler compounds are very similar chemically to our screened compounds and metallic, semi-metallic and semiconductors compounds are reported in this family. The results are presented in the figure 2 with the DOS at E_F for the considered ternary intermetallic compounds.

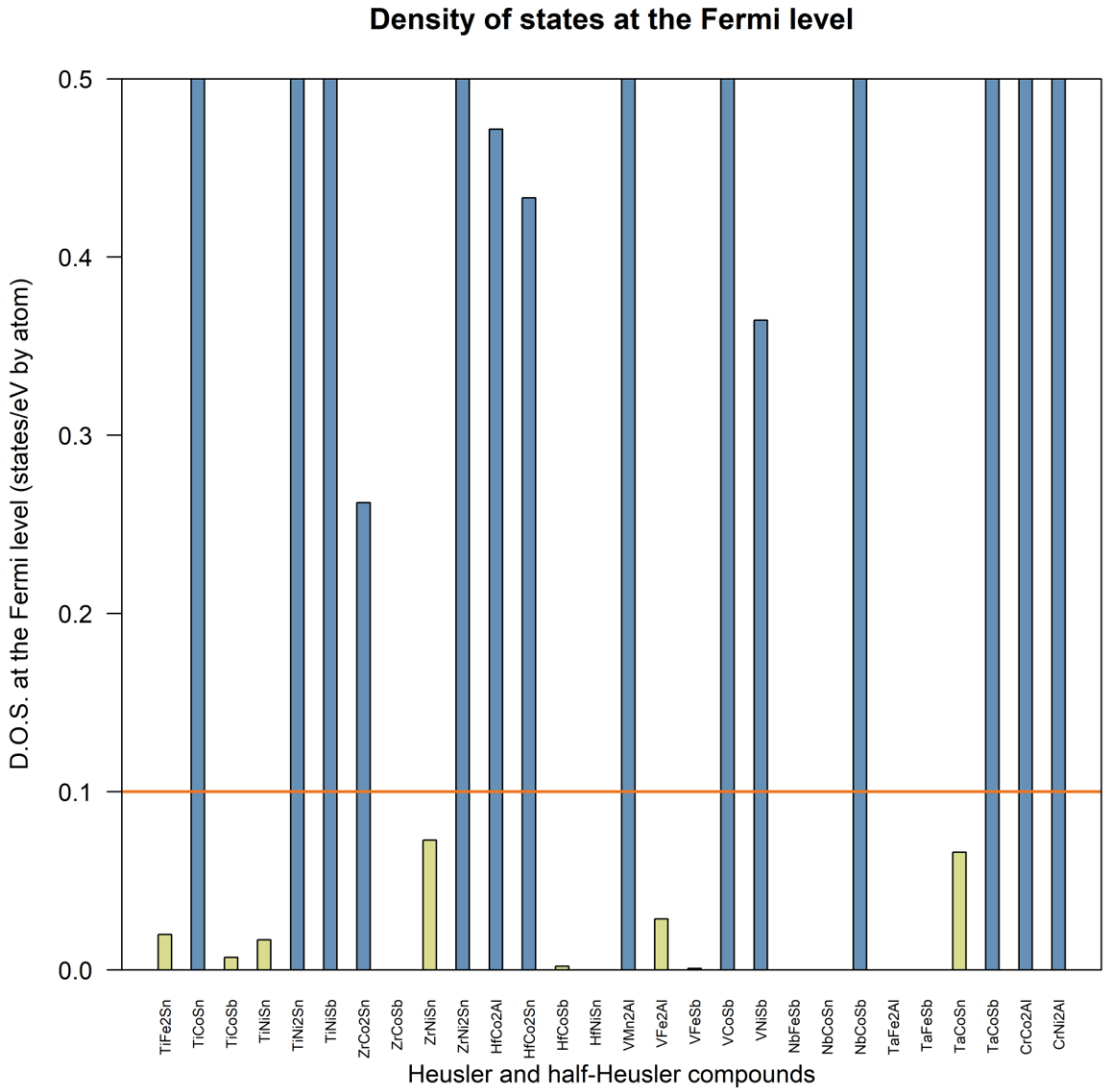

143

144 **Figure 2** : Density of states (DOS) at E_F for a selection of half-Heusler and Heusler compounds;
145 reported semiconductors and semi-metals are in yellow and metals are in blue.

146 As presented in ***Figure 2***, our discrimination criterion is efficient to sort metals for
147 semiconductors. Most of the reported semiconductors in the Heusler family exhibit a zero DOS
148 at E_F. However, some reported semiconductors or semi-metals do not and would be excluded
149 without our criterion, even though, according to the literature, they are promising thermoelectric
150 compounds. This is the case for ZrNiSn, TaCoSn or Fe_2VAl [36-39]. Indeed, ZrNiSn is a very good
151 example of both the necessity and the relevance of our discrimination criterion. As presented
152 **Figure *2***, the DOS(E_F) is equal to 0.07 states/eV by atom, which is not strictly zero, however

when looking at the density of states as a function of the energy, it is clear that the value falls down to zero in the vicinity of the Fermi energy (see figure 4 in reference [1]). A non-zero criterion is therefore essential to get rid of the calculation errors and uncertainties on both the density of states and the position of the Fermi level. Finally, our criterion allows to screen efficiently the Heusler family by excluding only metallic compounds. The robustness of our model being proven, another intermetallic family can be investigated.

Twelve selected compounds in the TiNiSi structure type

Among the 570 unique configurations calculated in the 4 structures type, 317 compounds are more stable in the TiNiSi structure-type than in any other structure type. But only 12 compounds are found to be non-metallic, according to the electronic criterion set at 0.1 state eV^{-1} by atom for the DOS at E_F. They are reported in Table 1. All of these compounds are mechanically stable (no imaginary frequency is observed in their phonon bands, figure S2).

Half-metals[40], which can be interesting for spintronic applications have also been searched. For these compounds, the majority-spin electrons are metallic whereas the minority-spin electrons are semiconducting. The criterion was applied to each spin directions. Eleven compounds complied with this criterion but only four are stable in the TiNiSi structure-type: CrNiSi, SrTiSn, BaVSb and BaCrSn (the DOS of these compounds are presented in figure S3 and phonon bands in figure S4). Nonetheless, these compounds are not interesting for thermoelectricity since they display a metallic total DOS and will not be investigated in detail in the following.

Table 1 *Non-metallic compounds in the TiNiSi structure type.*

***TMX* Compounds**	**Crystal databases**	**Enthalpy of formation (kJ mol^{-1})**	**DOS at the Fermi level (state. eV^{-1} by atom)**
TiCuSb	Unreported	-20.90	0.092

ZrZnSi	Unreported	-62.22	0.098
HfMnSb	Unreported	-26.15	0.098
HfCuSb	Unreported	-27.12	0.015
HfZnSi	Unreported	-52.84	0.098
TaCuSi	Unreported	-44.15	0.043
MoZnSi	Unreported	-15.53	0.062
TiMnSb	BeZrSi	-23.06	0.071
TiCoP	TiNiSi	-109.95	0.068
TiNiSi	TiNiSi	-88.47	0.061
HfCoP	TiNiSi	-109.99	0.032
TaNiP	TiNiSi	-73.48	0.062

We will first review the existence and structure of each selected compound. Then, for each candidate, a more specific study of the electronic structure will be presented. Finally, to assess their thermoelectric properties, the calculated values of the Seebeck coefficient and the thermal conductivity, will be examined.

Seven compounds among the 12 have not been reported in crystal structure databases. However, a careful study of phase diagrams may provide additional information. For the Ti-Cu-Sb, Zr-Zn-Si, Hf-Cu-Sb, and Ta-Cu-Si systems, no equimolar compound has been reported in the ternary phase diagram [41-45]. It is therefore unlikely that an equimolar compound is stable in the ternary orthorhombic structure, but it cannot be formally discarded. For the 3 other unreported compounds, HfMnSb, MoZnSi, and HfZnSi, no phase diagram is available for the corresponding systems, it is therefore difficult to conclude on their existence.

Among the 5 reported compounds, TiMnSb has been reported in the literature to crystallize in the BeZrSi structure type [46] in contrast with our calculations of a stable TiNiSi prototype. However, as discussed in our previous work [1], this discrepancy can be explained by the experimental conditions for the synthesis. Indeed, Noda *et al.* [46] have obtained TiMnSb under extreme conditions (high pressure and high temperature) possibly giving rise to a non-equilibrium phase.

Finally, four compounds are reported in the crystallographic databases in the orthorhombic TiNiSi structure. In the cases of TiCoP and TaNiP, the literature only deals with their crystal structure and there is no investigation of their electronic properties [47-48]. More information is provided for the other two compounds: TiNiSi and HfCoP. Recently, Huang *et al.* [49] investigated the thermoelectric properties of TiNiSi-based solid solutions. Theoretical results, based on DFT calculations with PBE-GGA, confirmed the presence of a pseudo-gap in the electronic band structure of TiNiSi. Measurements of the electric conductivity versus the temperature confirmed that TiNiSi is a semi-metal while thermoelectric properties were improved by the substitution of Ti by V [49]. These results confirm a previous report by Kong *et al.* [50] who have also highlighted the semi-metallic ground state of TiNiSi, thanks to their calculations. HfCoP, based on an extended Hückel calculation by Kleinke *et al.* [51], was considered as a metal. However, neither the electronic density of states nor the electrical resistivity was reported in this reference. The ground state of HfCoP is hence currently unknown.

Seebeck coefficient and lattice thermal conductivity at finite temperature

The Seebeck coefficient was calculated at finite temperatures within the semi-classical Boltzmann transport theory with the BoltzTrap package, assuming a constant relaxation time. The possibility of calculating the electronic thermal conductivity and electrical conductivity offered by the package was not implemented because these quantities depend on the electronic relaxation time, which then plays the role of an adjustable parameter. This is not the case for the Seebeck coefficient, which is independent on the relaxation time when it is assumed to be constant.

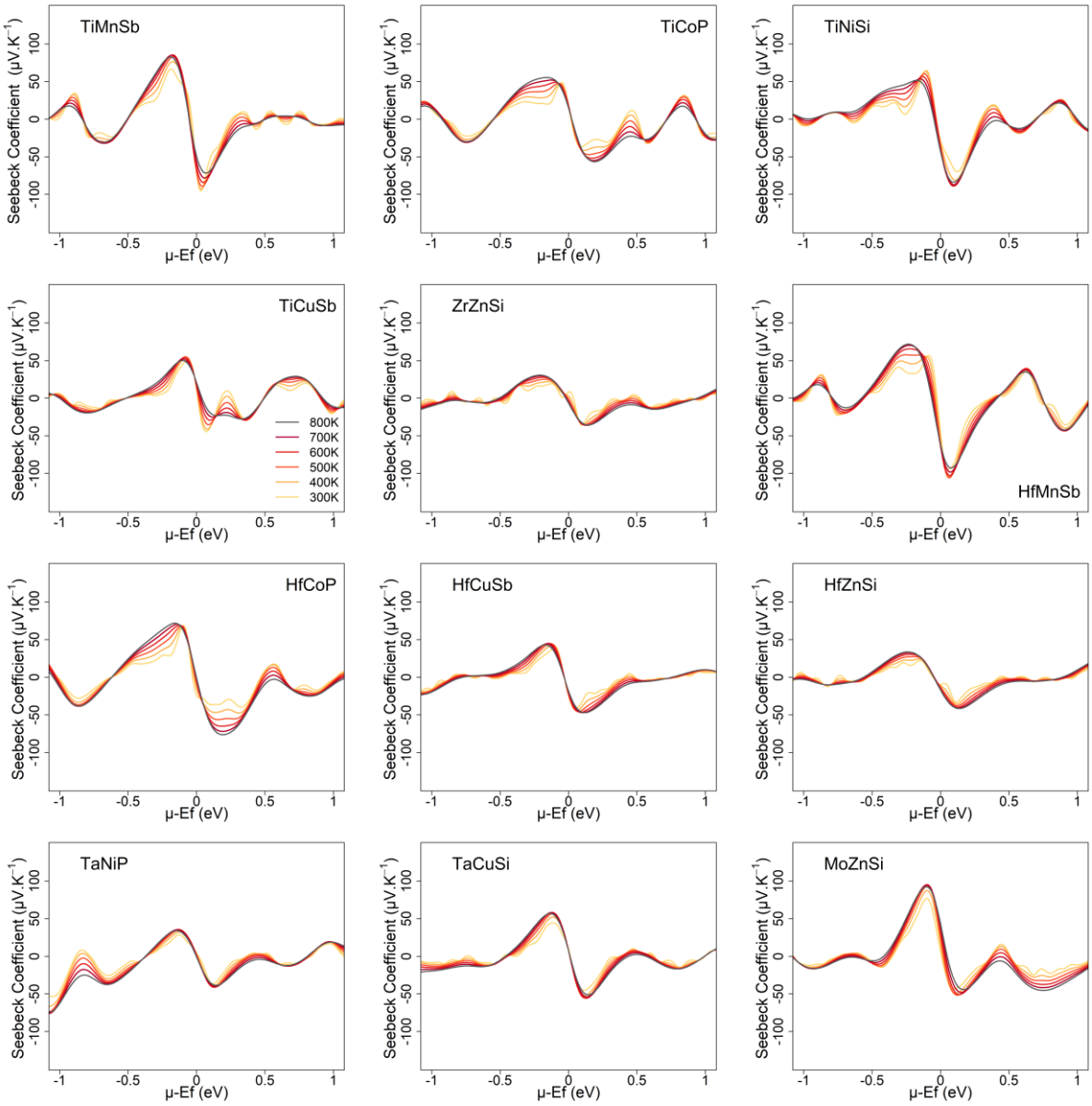

Figure 3. Calculated Seebeck coefficient as a function of the chemical potential for each compound. Each curve corresponds to a temperature varying by steps of 100K in the range 300 K (yellow) to 800 K (black).

The Seebeck coefficient has been plotted as a function of the chemical potential (μ) for each selected compound in the energy window [-1; +1 eV], which systematically covers the charge carrier concentration range [-10^{22} – 10^{22} cm^{-3}], well beyond the experimental doping concentrations conventionally achieved. Figure 3 presents for each compound the variations of *S* for several temperatures varying by steps of 100 K in the range 300 K and 800 K. For the positive values of the Seebeck coefficient, increase with the temperature rise is generally observed. Only, TiNiSi and TiCuSb exhibit a different behaviour with Seebeck coefficient at

300 K higher than at 800 K. Even though this trend is maintained for the negative Seebeck coefficient, with the absolute value at 800 K higher than at 300 K, four compounds exhibit an opposite behaviour, TiMnSb, TiCuSb, MoZnSi and HfMnSb.

Several compounds like ZrZnSi or HfZnSi do not show values of the Seebeck coefficient larger than ± 50 μV K^{-1} and therefore do not seem to be very promising in contrast with TiMnSb or MoZnSi for example. First extremum of the calculated Seebeck coefficient close to the Fermi level are listed in Table 2. In this table, values at 700 K are reported, to compare the compounds in the same way as it will be done for the lattice thermal conductivity (values at 300 K are reported in table S2). We choose to focus on the maximal values of the Seebeck coefficient when μ is near the Fermi level for an easy comparison.

Table 2. Values of the first extremum of the calculated Seebeck coefficient close to the Fermi level and Slack's lattice thermal conductivity at 700 K for the TiNiSi compounds.

***TMX* compounds**	**S_{max} (μV K^{-1}) > 0 (700K)**	**S_{max} (μV K^{-1}) < 0 (700K)**	**Slack's lattice Thermal conductivity at 700K (W m^{-1} K^{-1})**
TiMnSb	85	-78	5.4
TiCoP	52	-55	15.7
TiNiSi	54	-87	13.7
TiCuSb	52	-28	3.9
ZrZnSi	30	-36	9.9
HfMnSb	70	-98	6.1
HfCoP	71	-72	11.6
HfCuSb	44	-47	3.7
HfZnSi	33	-41	7.4
TaNiP	41	-76	7.6
TaCuSi	58	-54	9.7
MoZnSi	95	-48	6.5

As mentioned before, ZrNiSi, HfZnSi, HfCuSb, and TaCuSi present quite low Seebeck coefficient near the Fermi energy, regardless their conduction type. Considering both positive and negative values, TiMnSb and HfMnSb can be considered as the best compounds when other compounds could be promising at most in one of the two conduction types. For example, TiNiSi has a negative Seebeck coefficient twice as large as its positive counterpart whereas it is the

opposite for MoZnSi. These results are comparable at other temperatures where similar trend can be noticed (table S2). No clear tendencies can be noticed in the evolution of the Seebeck coefficient regarding the nature of each *T*, *M* or *X* element in these compounds.

Lattice thermal conductivity, which is essential for the determination of *ZT*, can be estimated by the Slack's equation [11-12] by assuming that heat is conducted only by acoustic phonons [52-53], through the equation 2:

$$K_L = 3.1 \times 10^{-6} \frac{M\,\theta_D^3 \delta}{\gamma^2 n^{\frac{2}{3}} T} \qquad \textbf{(2)}$$

where θ_D is the Debye temperature in K, δ^3 is the volume per atom in Å^3, n is the number of atoms in the primitive unit cell, M_{av} is the average atomic mass in the atomic unit and γ is the average Grüneisen parameter. The Debye temperature and the Grüneisen parameter are evaluated from the transverse and longitudinal sound velocity, which are obtained from the calculated elastic modulus. The calculated elastic properties (table S3) have been obtained from the phonon calculations for each compound (see figure S2). Slack's model neglects the transport of heat by optical phonons and this could lead to underestimated values of lattice thermal conductivity. However, it also assumes that the acoustic phonons are scattered only by acoustic phonons, neglecting all the other scattering mechanisms (isotopes, impurities, vacancies, charge carriers, dislocations, grain boundaries, crystal boundaries, etc.) This last approximation has the strongest impact on Slack's values [12], which are systematically overestimated (up to an order of magnitude) as soon as the relative atomic mass difference of the constituting elements is larger than roughly ~ 100% [12]: this condition is indeed fulfilled for the 12 screened compounds. Despite these drawbacks, Slack's model provides reliable trends at temperatures larger than the Debye temperature, when phonon – phonon scattering dominates over the other scattering processes. To fulfil this condition for all the compounds, the values presented in Table 2 were calculated at 700 K.

The range of lattice thermal conductivity values is quite broad with estimated values between 3 and 15 W m^{-1} K^{-1} which cannot be compared to experimental values due to lack of data. These values are quite large compared to the best thermoelectric materials such as Bi_2Te_3 or Sb_2Te_3 which exhibit low thermal lattice thermal conductivity (~ 2 W m^{-1} K^{-1}) [54]. They are, nonetheless, still promising because they were calculated for a perfect crystal and thus as above discussed, overestimated. Moreover, it is known that defects or impurities can strongly decrease the lattice thermal conductivity. For instance, the half-Heusler HfNiSn displays a thermal conductivity of 10 W m^{-1} K^{-1} at 300 K [55] while the solid solution $Hf_{0.75}Zr_{0.25}NiSn_{0.99}Sb_{0.02}$displays a thermal conductivity of 5 W m^{-1} K^{-1} at 300 K and ZT = 0.9 at 800 K [56].

Keeping the ***X***-element constant and considering the ***T*** element, as expected, the lattice thermal conductivity is, in general, lower for "heavier" ***T*** in the same columns of the periodic table as for ***T***CuSb or ***T***CoP. In the case of ***T***MnSb, the trend is reversed as κ_L(TiMnSb) is lower than κ_L(HfMnSb). Keeping the *T* element constant and considering the *X* element, we noticed that the antimonides present the lowest thermal conductivity compared to the silicides or the phosphides, in accordance with the larger atomic mass of antimony.

DISCUSSION

Keeping in mind that the values presented here are from calculations based on DFT-PBE and constant relaxation time approximation implemented in a perfect crystal, our study offers the possibility to identify the most promising compounds among the 12 selected TiNiSi-type compounds from our screening of 570 possible compositions. For example according to Table 2, even though, lattice thermal conductivity is quite low for the two ***T***CuSb compounds, their Seebeck coefficients are also systematically low. ZrNiSi and TaCuSi exhibit also low Seebeck coefficient, which are for these compounds accompanied by high lattice thermal conductivity values. Thus, if one adds to these low values the fact that, according to the reported ternary

phase diagram, these four compounds are not stable, it is probably not worth trying their synthesis.

On the other hand, HfMnSb and MoZnSi combine large Seebeck coefficients and a small lattice thermal conductivity that could lead to interesting properties. Nonetheless, their existence is not established.

Regarding the four compounds which have already been reported in the literature, a ranking is also possible. The highest value of the Seebeck coefficient is reached in TiNiSi, which has already been reported as interesting for its thermoelectric properties in the solid solution $Ti_{1-x}V_xNiSi$ [49]. The presently calculated values of the Seebeck coefficient seem to confirm the calculated values calculated by Huang *et al.* [49], with $S \approx \pm 65$ μV. K^{-1} at 300 K for both type of charge carrier whereas our calculation gives $S = 64$ μV. K^{-1} and $S = -69$ μV. K^{-1} at 300 K. However, the measured values (-16 μV. K^{-1} at 300K) in Ref. [49] differ from the calculated one, but this difference can be explained by the charge carrier concentration of the pristine TiNiSi, which is around 2×10^{21} cm^{-3}. This relatively large value indicates the presence of intrinsic defects in the sample. Finally, HfCoP seems to be more interesting than TiCoP as its Seebeck coefficient is larger and associated with a lower lattice thermal conductivity. TaNiP exhibits the lowest lattice thermal conductivity of the four reported compounds and negative Seebeck coefficient of the same order of magnitude as in HfCoP.

CONCLUSION

After determining the stability of thousands of *TMX* compositions in 4 structure types, a more focused investigation has been undertaken on the compounds which crystallize in the TiNiSi structure type. In a second stage, the electronic band structure has been examined and an effective criterion of the DOS at the Fermi level has been established by comparing calculated DOS of known semiconducting elements and compounds. Then, this empirical criterion of 0.1

state eV^{-1} by atom has been applied to the *TMX* compounds, stable in the orthorhombic structure. It has led to the selection of 12 non-metallic compounds among the 317 possible compounds while it was commonly admitted that all the TiNiSi are metallic [57]. Additional phonon and BoltzTrap calculations allowed to rank the 12 selected compounds to identify those which are the most interesting to be synthesized from the point of view of their anticipated thermoelectric properties. Although MoZnSi could be an interesting compound as it presents the highest Seebeck coefficient associated with a small lattice thermal conductivity, there is no information about its possible stability. So, it seems more relevant to focus on HfCoP and TaNiP as starting points. Both compounds are already reported in the literature as crystallizing in the TiNiSi structure type [48, 51] and present the best compromise between high Seebeck coefficient and a low lattice thermal conductivity.

ACKNOWLEDGEMENTS

DFT calculations were performed using HPC resources from GENCI-CINES (Grant 2019-A0060906175) and financial support from the Agence Nationale de la Recherche is acknowledged (ANR-18-CE05-0010-01).

SUPPORTING INFORMATION AVAILABLE

Table S1: Elemental, binaries and ternaries compounds information's

Figure S1: Electronic density of states for the twelve TMX compounds calculated by DFT using GGA-PBE approximation. The Fermi level is chosen as the origin of energies. The discrimination criterion is represented by the red dotted line.

Figure S2: Phonon curves dispersion of the twelve TMX compounds calculated using the Phonopy code.

Figure S3: Electronic density of states for the four (half-metals) *TMX* compounds calculated by DFT using GGA-PBE approximation. The Fermi level is chosen as the origin of energies. Both spin directions are presented.

Figure S4: Phonon curves dispersion of the four (half-metals) *TMX* compounds calculated using the Phonopy code.

Table S2: Values of the first extremum of the calculated Seebeck coefficient close to the Fermi level at 300 K for the TiNiSi compounds.

Table S3: The bulk modulus (B), shear modulus (G), Young's modulus (E) and Poisson ratio (ν) of the screened TMX compounds.

REFERENCES

1. Barreteau, C.; Crivello, J.-C.; Joubert, J.-M.; Alleno, E., Looking for new thermoelectric materials among TMX intermetallics using high-throughput calculations. *Comput. Mater. Sci* **2019,** *156*, 96-103.
2. Villars, P.; Cenzual, K., Pearson's Crystal Data: Crystal structure database for inorganic compounds. International, A., Ed. Materials Park: Ohio, USA, 2017/2018.
3. Belsky, A.; Hellenbrandt, M.; Karen, V. L.; Luksch, P., New developments in the Inorganic Crystal Structure Database (ICSD): accessibility in support materials research and design. *Acta Crystallogr. B* **2002,** *58*, 364-369.
4. Feng, Z.; Fu, Y.; Putatunda, A.; Zhang, Y.; Singh, D. J., Electronic structure as a guide in screening for potential thermoelectrics: demonstration for half-Heusler compounds. *Phys. Rev. B* **2019,** *100*, 085202.
5. Guo, S.; Jia, T.-T.; Zhang, Y., Electrical properties dominated promising half-Heusler thermoelectrics through high-throughput materials computations. *J. Phys. Chem. C* **2019,** *123*, 18824-18833.
6. Legrain, F.; Carrete, J.; van Roekeghem, A.; Madsen, G. K. H.; Mingo, N., Materials screening for the discovery of new half-Heuslers: Machine learning versus *ab initio* methods. *J. Phys. Chem. B* **2017,** *122*, 625-632.
7. Ma, J.; Hegde, V. I.; Munira, K.; Xie, Y.; Keshavarz, S.; Mildebrath, D. T.; Wolverton, C.; Ghosh, A. W.; Butler, W. H., Computational investigation of half-Heusler compounds for spintronics applications. *Phys. Rev. B* **2017,** *95*, 024411.
8. Zeeshan, M.; Singh, H. K.; van den Brink, J.; Kandpal, H. C., *Ab initio* design of new cobalt-based half-Heusler materials for thermoelectric applications. *Phys. Rev. Mater.* **2017,** *1*, 075407.
9. Madsen, G. K. H.; Singh, A. K., BoltzTrap. A code for calculating band-structure dependent quantities. *Comput. Phys. Comm.* **2006,** *175*, 67-71.
10. Madsen, G. K. H.; Carrete, J.; Verstraete, M. J., BoltzTrap2, a program for interpolating ban structures and calculating semi-classical transport coefficients. *Comput. Phys. Comm.* **2018,** *231*, 140-145.

11. Slack, G. A., Nonmetallic crystals with high thermal conductivity. *J. Phys. Chem. Solids* **1973,** *34*, 321-335.
12. Slack, G. A., The thermal conductivity of nonmetallic crystals. *Solid State Physics* **1979,** *34*, 1-71.
13. Kresse, G.; Hafner, J., *Ab-initio* molecular dynamics for liquid metals. *Phys. Rev. B* **1993,** *47*, 558(R).
14. Kresse, G.; Joubert, D., From ultrasoft pseudopotentials to the projector augmented-wave method. *Phys. Rev. B* **1999,** *59* (3), 1758-1775.
15. Kresse, G.; Furthmüller, J., Efficient iterative schemes for an *ab-initio* total-energy calculations using plane-wave basis set. *Phys. Rev. B* **1996,** *54*, 11169-11186.
16. Hafner, J.; Kresse, G.; Vogtenhuber, D.; Marsman, M. The Vienne *Ab-Initio* Simulation Package (VASP).
17. Perdew, J. P.; Burke, K.; Ernzerhof, M., Generalized gradient approximation made simple. *Phys. Rev. Lett.* **1996,** *77*, 3865-3868.
18. Blöchl, P. E.; Jepsen, O.; Andersen, O. K., Improved tetrahedron method for Brillouin-zone integrations. *Phys. Rev. B* **1994,** *49* (23), 16223-16233.
19. Parlinski, K.; Li, Z. Q.; Kawazoe, Y., First-principles determination of the soft mode in cubic ZrO_2. *Phys. Rev. Lett.* **1997,** *78*, 4063-4066.
20. Togo, A.; Tanaka, I., First-principles phonon calculations in materials science. *Scr. Mater.* **2015,** *108*, 1-5.
21. Togo, A.; Oba, F.; Tanaka, I., First-principles calculations of the ferroelastic transition between rutile-type and $CaCl_2$-type SiO_2 at high pressures *Phys. Rev. B* **2008,** *78*, 134106.
22. Ashcroft, N. W.; Mermin, N. D., *Solid State Physics*. Saunders College Publishing: Orlando, 1976.
23. Tran, F.; Blaha, P., Importance of the kinetic energy density for band gap calculations in solids with density functional theory. *J. Phys. Chem. A* **2017,** *121*, 3318-3325.
24. Yakovkin, I. N.; Dowben, P. A., The problem of the band gap in LDA calculations. *Surface Review and Letters* **2007,** *14* (3), 481-487.
25. Greiner, E. S.; Gutowski, J. A., Electrical Resistivity of Boron. *J. Appl. Phys.* **1957,** *28*, 1364-1365.
26. Yu, C.; Liu, J.; Lu, H.; Chen, J., Ab initio calculation of the properties and pressure induced transition of Sn. *Sol. State. Commun.* **2006,** *140*, 538-543.
27. Busch, G. A.; Kern, R., Seminducting properties of gray tin. *Sol. Stat. Phys.* **1960,** *11*, 1-40.
28. Goodman, N. B.; Ley, L.; Bullett, D. W., Valence-band structures of phosphorus allotropes. *Phys. Rev. B* **1983,** *27*, 7440-7450.
29. Reitz, J. R., Electronic band strucuture of Selenium and Tellurium. *Phys. Rev.* **1957,** *105*, 1233-1240.
30. Gaspar, R., Electronic structure of semi-conducting selenium and tellurium. *Acta Physica* **1957,** *7*, 289-311.
31. Loucks, T. L.; Cutler, P. H., Band structure and Fermi surface of Beryllium. *Phys. Rev.* **1964,** *133*, A819-A829.
32. Mitchell, M. A., Electrical resistivity of beryllium. *J. Appl. Phys.* **1975,** *46*, 4742-4746.
33. Chou, M. Y.; Lam, P. K.; Cohen, M. L., *Ab initio* study of structural and electronic properties of beryllium. *Phys. Rev. B* **1983,** *28*, 4179-4185.
34. Papaconstantopoulo, D. A., *Handbook of the band structure of elemental solids*. Springer US: 2015; Vol. 3, p 655.
35. Gillessen, M.; Dronskowski, R., A combinatorial study of full Heusler alloys by first-principles computational methods. *J. Comput. Chem.* **2009,** *30*, 1290-1299.
36. Li, S.; Zhu, H.; Mao, J.; Feng, Z.; Li, X.; Chen, C.; Cao, F.; Liu, X. J.; Singh, D. J.; Ren, Z.; Zhang, Q., n-type TaCoSn-based half-Heusler as promising thermoelectric materials. *Appl. Mater. Interfaces* **2019,** *11*, 41321-41329.
37. Maier, S.; Denis, S.; Adam, S.; Crivello, J.-C.; Joubert, J. M.; Alleno, E., Order-disorder transitions in the Fe_2VAl Hesuler alloy. *Acta Materialia* **2016,** *121*, 126-136.

38. Kuentzler, R.; Clad, R.; Schmerber, G.; Dossmann, Y., Gap at the Fermi level and magnetism in RMSn ternary compounds (R= Ti, Zr, Hf and M= Fe, Co, Ni). *J. Magn. Magn. Mater.* **1992,** *104-107*, 1976-1978.
39. Hu, T.; Yang, D.; Su, X.; Yan, Y.; You, Y.; Liu, W.; Uher, C.; Tang, X. F., Interpreting the combustion process for high-performance ZrNiSn thermoelectric materials. *ACS Appl. Mater. Interfaces* **2018,** *10*, 864-872.
40. de Groot, R. A.; Mueller, F. M.; van Engen, P. G.; Buschow, K. H. J., New class of materials: half-metallic ferromagnets. *Phys. Rev. Lett.* **1983,** *50*, 2024-2027.
41. Dolotko, O. V.; Dmytriv, G. S.; Pavlyuk, V. V., Interaction of Components in the Zr-Zn-Si System at 600 °C. *Pol. J. Chem.* **2001,** *75*, 453-455.
42. Kobluyk, N. A.; Romaka, L. P.; Bodak, O. I., Interaction between the components in the Ti-Cu-Sb system at 770 K. *J. Alloys Compd.* **2000,** *309*, 176-178.
43. Melnychenko-Koblyuk, N.; Romaka, L.; Akselrud, L. G.; Romaka, V. V.; Stadnyk, Y., Interaction between components in Hf-Cu-Sb ternary system at 770K. *J. Alloys Compd.* **2008,** *461*, 147-149.
44. Savitskii, E. M.; Efimov, Y. V.; Frolova, T. M., Copper effect on structure and superconductive properties of transition metal silicides [V(Nb, Ta, Cr, Mo, W)-Si-Cu alloy systems]. *Izv. Akad. Nauk SSSR, Neorg. Mater.* **1979,** *15*, 654-657.
45. Reid, J. S.; Kolawa, E.; Nicolet, M.-A., Thermodynamics of (Cr, Mo, Nb, Ta, V or W)-Si-Cu ternary systems. *J. Mater. Res.* **1992,** *7* (9), 2424-2428.
46. Noda, Y.; Shimada, M.; Koizumi, M., High-pressure synthesis and magnetic properties of MMnSb (M= Ti, V, Cr) with Ni_2In type structures. *Inorg. Chem.* **1984,** *23*, 628-630.
47. Rundqvist, S.; Nawapong, P. C., The Crystal Structure of ZrFeP and Related Compounds. *Acta Chem. Scand.* **1966,** *20*, 2250-2254.
48. Lomnytska, Y. F.; Agatinskaya, L. P.; Kuz'ma, Y. B., Component interaction in the system titanium-cobalt-phosphorus. *Sov. Prog. Chem.* **1981,** *47*, 29-32.
49. Huang, Y.; Nagai, H.; Hayashi, K.; Miyazaki, Y., Preparation and thermoelectric properties of pseudogap intermetallic $(Ti_{1-x}V_x)NiSi$ solid solutions. *J. Alloys Compd.* **2019,** *771*, 111-116.
50. Kong, B.; Chen, X.-R.; Cai, L.-C.; Zhu, J., Structural and elastic properties of typical equiatomic ternary intermetallic compound TiNiSi under pressure. *Physica B: Condensed Matter* **2010,** *405* (6), 1591-1595.
51. Kleinke, H.; Franzen, H. F., Synthesis Crystal Structure and Properties of HfM'P (M'= Fe, Co, Ni) in Comparison to ZrNiP. *Z. Anorg. Allg. Chem.* **1996,** *622*, 1893-1900
52. Hou, Z.; Takagiwa, Y.; Shinohara, Y.; Xu, Y.; Tsuda, K., Machine-Learning-assisted development and theoritical consideration for the $Al_2Fe_3Si_3$ thermoelectric material. *Appl. Mater. Interfaces* **2019,** *11*, 11545-11554.
53. Shiota, Y.; Muta, H.; Yamamoto, K.; Ohishi, Y.; Kurosaki, K.; Yamanaka, S., A new semiconductor $Al_2Fe_3Si_3$ with complex crystal structure. *Intermetallics* **2017,** *89*, 51-56.
54. Elsheikh, M. H.; Shnawah, D. A.; Sabri, M. F. M.; Said, S. B. M.; Hassan, M. H.; Bashir, M. B. A.; M., M., A review on thermoelectric renewable energy: Principle parameters that affect their performance. *Renewable and Sustainable Energy Reviews* **2014,** *30*, 331-355.
55. Uher, C.; Yang, J.; Hu, S.; Morelli, D. T.; Meisner, G. P., Transport properties of pure and doped MNiSn (M=Zr, Hf). *Phys. Rev. B* **1999,** *59*, 8615.
56. Yan, X.; Joshi, G.; Liu, W.; Lan, Y.; Wang, H.; Lee, S.; Simonson, J. W.; Poon, S. J.; Tritt, T. M.; Chen, G.; Ren, Z. F., Enhanced Thermoelectric Figure of Merit of p-Type Half-Heuslers. *Nano Letters* **2011,** *11*, 556.
57. Landrum, G. A.; Hoffmann, R. D.; Evers, J.; Boysen, H., The TiNiSi Family of Compounds: Structure and Bonding. *Inorg. Chem.* **1998,** *37*, 5754-5763.

TABLE OF CONTENTS

488

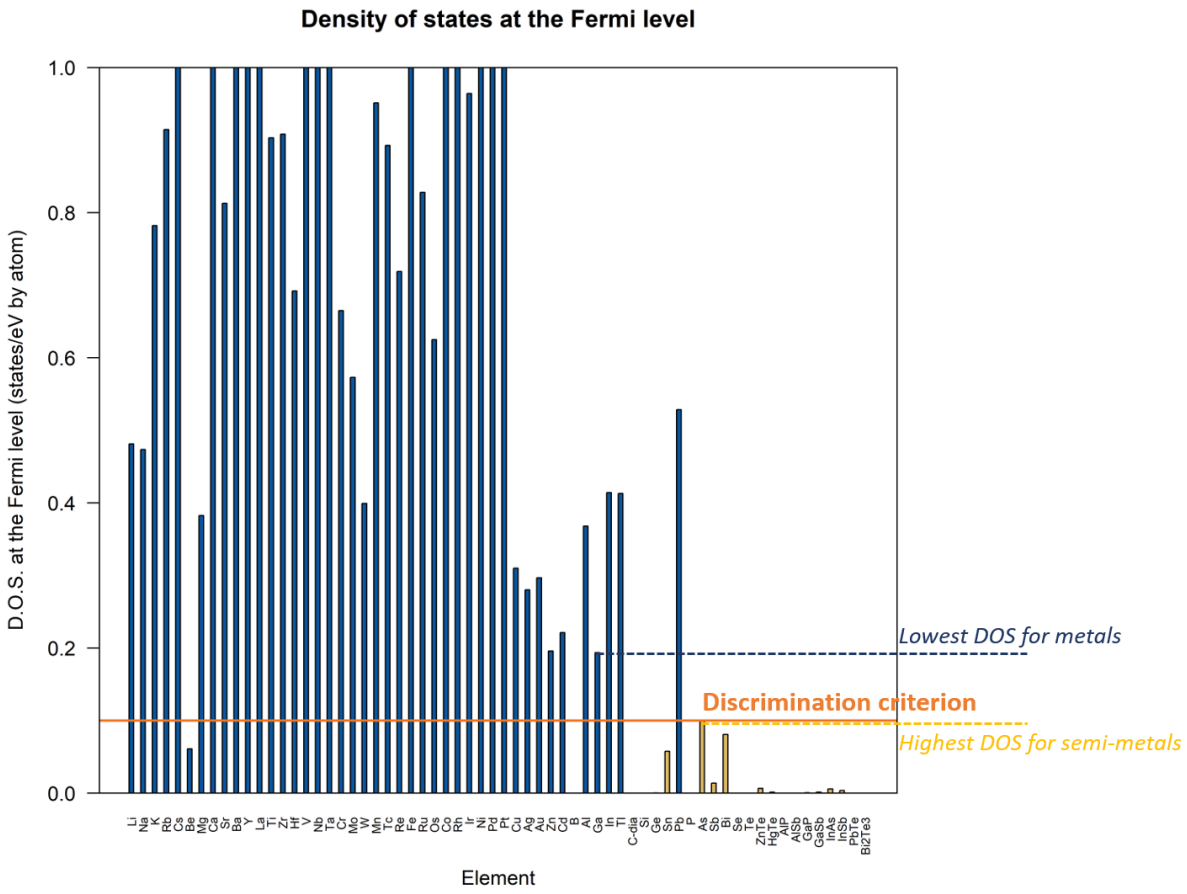

489

490 Figure 1

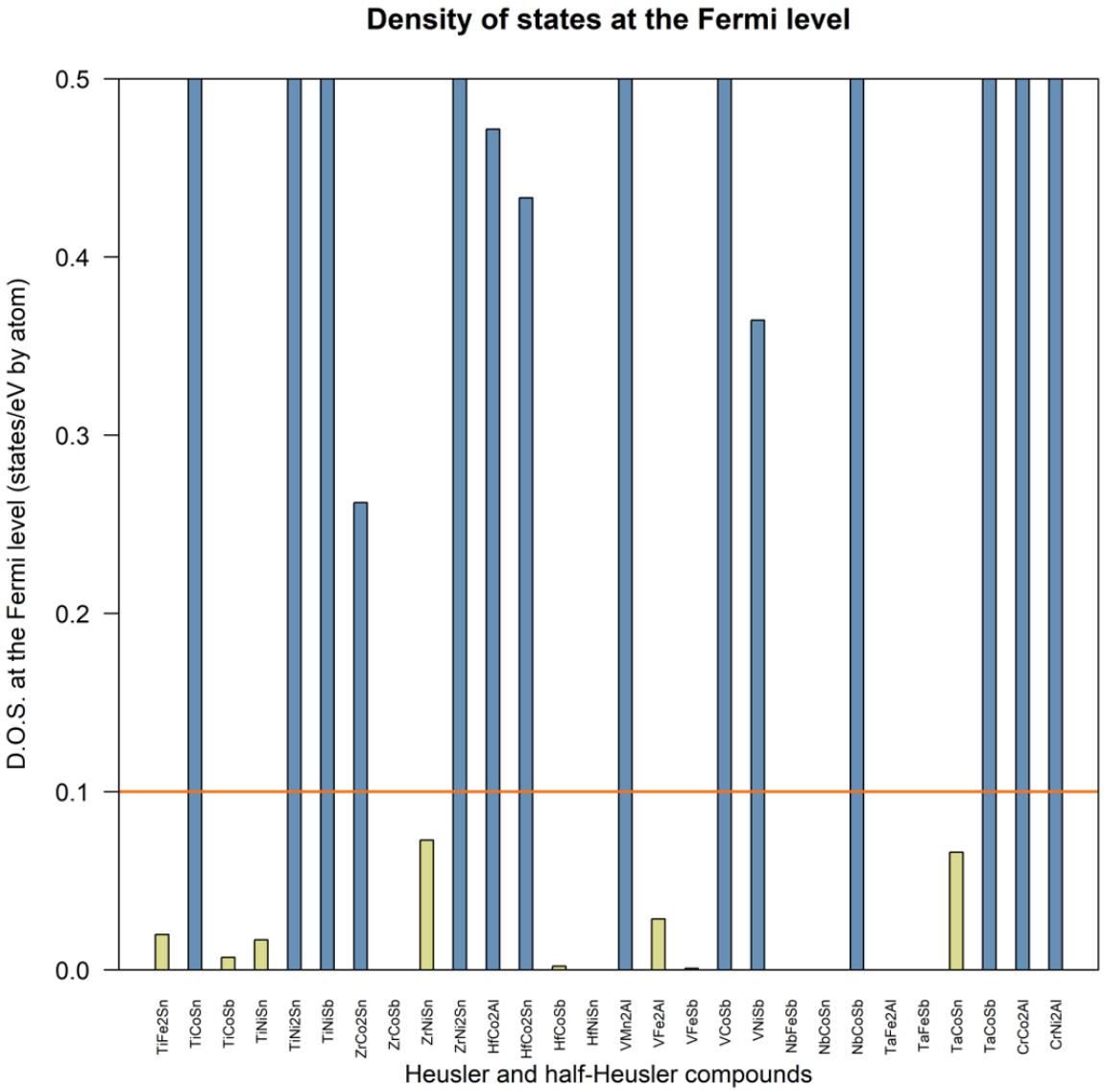

491

492 Figure 2

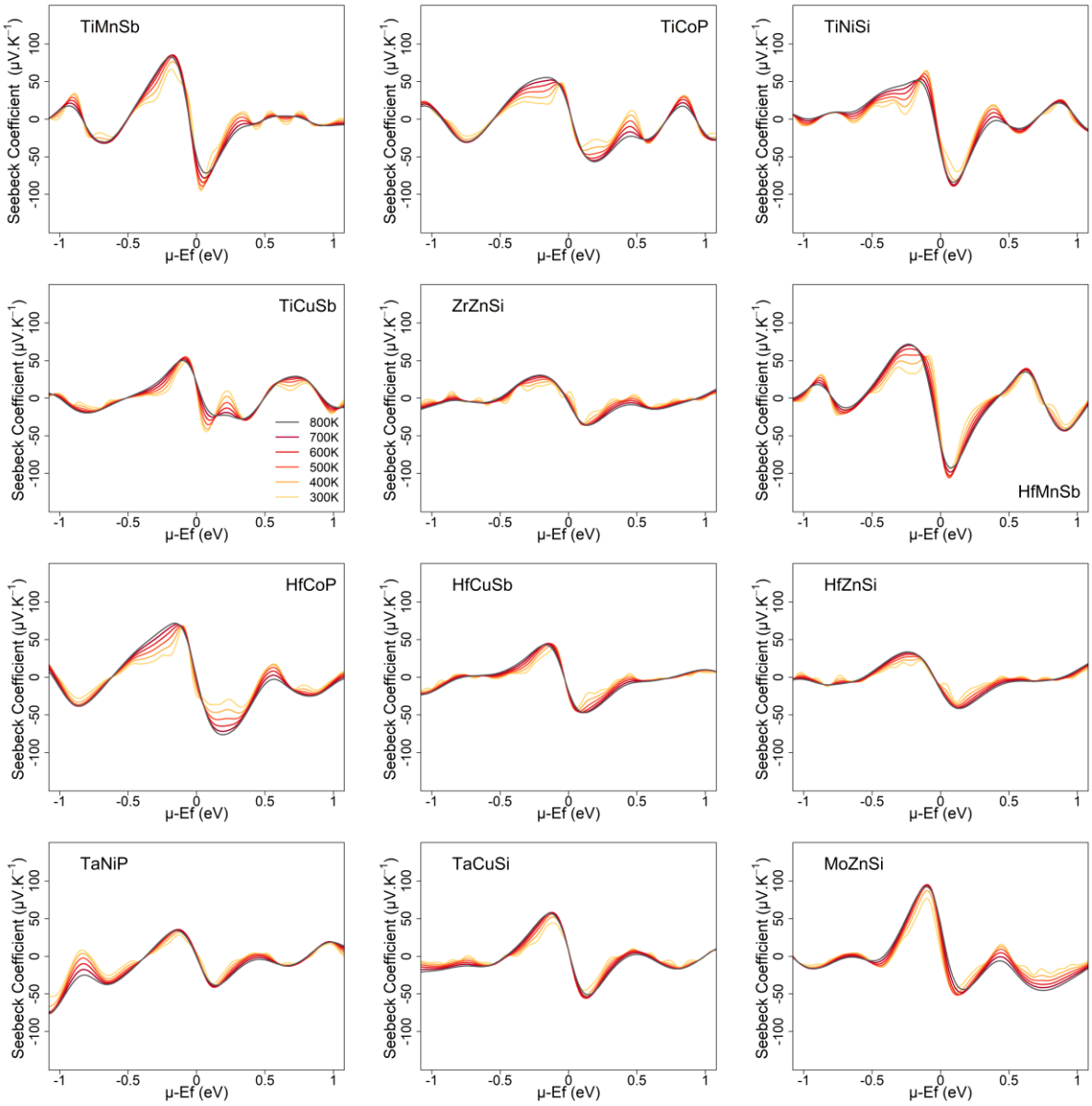
TiMnSb
TiCoP
TiNiSi
TiCuSb
ZrZnSi
HfMnSb
HfCoP
HfCuSb
HfZnSi
TaNiP
TaCuSi
MoZnSi
Seebeck Coefficient (μV.K⁻¹)
μ-Ef (eV)
800K
700K
600K
500K
400K
300K

Figure 3

504 Table 1

TMX Compounds	Crystal databases	Enthalpy of formation (kJ mol^{-1})	DOS at the Fermi level (state. eV^{-1} by atom)
TiCuSb	Unreported	-20.90	0.092
ZrZnSi	Unreported	-62.22	0.098
HfMnSb	Unreported	-26.15	0.098
HfCuSb	Unreported	-27.12	0.015
HfZnSi	Unreported	-52.84	0.098
TaCuSi	Unreported	-44.15	0.043
MoZnSi	Unreported	-15.53	0.062
TiMnSb	BeZrSi	-23.06	0.071
TiCoP	TiNiSi	-109.95	0.068
TiNiSi	TiNiSi	-88.47	0.061
HfCoP	TiNiSi	-109.99	0.032
TaNiP	TiNiSi	-73.48	0.062

505

506

507 Table 2

TMX compounds	S_{max} (μV K^{-1}) > 0 (700K)	S_{max} (μV K^{-1}) < 0 (700K)	Slack's lattice Thermal conductivity at 700K (W m^{-1} K^{-1})
TiMnSb	85	-78	5.4
TiCoP	52	-55	15.7
TiNiSi	54	-87	13.7
TiCuSb	52	-28	3.9
ZrZnSi	30	-36	9.9
HfMnSb	70	-98	6.1
HfCoP	71	-72	11.6
HfCuSb	44	-47	3.7
HfZnSi	33	-41	7.4
TaNiP	41	-76	7.6
TaCuSi	58	-54	9.7
MoZnSi	95	-48	6.5

508

509

510

511